Graphical Abstract

Synthesis and characterization of novel diazenes bearing pyrrole, thiophene and thiazole heterocycles as efficient photochromic and nonlinear optical (NLO) materials

M. Manuela M. Raposo, A. Maurício C. Fonseca, M. Cidália R. Castro, M. Belsley, M. Fátima S. Cardoso, Luís M. Carvalho and Paulo J. Coelho

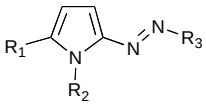

R_1 = H, thienyl
R_2 = alkyl, aryl
R_3 = aryl, thiazolyl

Synthesis and characterization of novel diazenes bearing pyrrole, thiophene and thiazole heterocycles as efficient photochromic and nonlinear optical (NLO) materials

M. Manuela M. Raposo,[a] * A. Maurício C. Fonseca,[a] M. Cidália R. Castro,[a] M. Belsley,[b] M. Fátima S. Cardoso,[b] Luís M. Carvalho[c] and Paulo J. Coelho[c]

[a] *Center of Chemistry, University of Minho, Campus de Gualtar, 4710-057 Braga, Portugal*

[b] *Center of Physics, University of Minho, Campus de Gualtar, 4710-057 Braga, Portugal*

[c] *Center of Chemistry, University of Trás-os-Montes and Alto Douro, 5001-801 Vila Real, Portugal*

Dedicated to the Centenary of the Portuguese Chemical Society

[*]Corresponding author. Tel: + 351 253 604381; Fax: +351 253 604382; *e-mail:* mfox@quimica.uminho.pt

Abstract- Two series of novel thermally stable second-order nonlinear optical (NLO) and photochromic chromophores have been designed and synthesized. The two series of compounds were based on different combinations of donor groups (pyrrole or thienylpyrrole) which act simultaneously as π-conjugated bridges, together with diazoaryl or diazothiazolyl as acceptor moieties. Their photochromic and electrochemical behavior were characterized, while hyper-Rayleigh scattering (HRS) was employed to evaluate their second-order nonlinear optical properties. The results of these studies have been critically analyzed together with two other related compounds reported earlier from our laboratories in which the thienylpyrrole system was used as the donor group keeping the functionalized diazoaryl as acceptor moiety. The measured molecular first hyperpolarizabilities and the observed photochromic behavior showed strong variations for the different donor systems used (pyrrole or thienylpyrrole) and were also sensitive to the acceptor strength of the diazenehetero(aryl) moiety.

The thienylpyrrole based compounds endowed with extended π-conjugated bridges and stronger donor auxiliary effects in comparison to the pyrrole compounds, when coupled to the stronger acceptor diazo(hetero)aryl groups gave rise to significantly larger hyperpolarizabilities (β = 274 - 415 x 10^{-30} esu) for an incident wavelength of 1064nm). These compounds also displayed improved photochromic behavior with very fast response to the visible light stimulus (1.5 s) and fast thermal return to the original forms (2-3 s).

Keywords: thiazole, heterocyclic azo dyes, donor-acceptor chromophores, solvatochromic probes, hyper-Rayleigh scattering (HRS), Nonlinear optical (NLO) materials, redox potentials, photochromism, thermal stability

1. Introduction

Although the search for organic molecules with strong nonlinear optical (NLO) response has been the focus of intense research for many years, their potential for improving a variety of opto-electronic applications ranging from optical data transmission to information processing, has only been partially realized. Candidate molecules for NLO applications should possess large molecular hyperpolarizabilities and low optical losses within the spectral region of interest. A general approach for obtaining materials with important nonlinear optical properties consists in the synthesis of chromophores involving electron-donor and electron-acceptor groups linked through a π-conjugated spacer, so called D-π-A systems [1]. The efficient intramolecular charge transfer (ICT) along the π-conjugated bridges of these organic systems is particularly relevant in the development of NLO materials since, amongst other properties, it can promote large optical nonlinearities and ultra-fast responses, in particular a nearly instantaneous electronic polarization. For these systems, optimization of the π-conjugated bridges, electron-donor and electron-acceptor characteristics of the substituents are needed to obtain the highest nonlinearities at a molecular level [2].

One approach currently being explored by many researchers is to substitute the benzene rings typical of these D-π-A systems with an electron rich and/or electron poor aromatic ring that can act as an auxiliary donor/acceptor while modulating the π-conjugated bridges. Experimental studies have demonstrated that replacing the benzene ring of a chromophore with easily delocalizable five-membered heteroaromatic rings, such as thiophene, pyrrole and thiazole, results in an enhanced molecular hyperpolarizability [3]. Recent theoretical calculations suggest that heterocyclic rings play a subtle role in the second-order NLO properties of donor-acceptor compounds. In fact, the increase or decrease of the molecular nonlinear activity of these heteroaromatic systems depends not only on the electronic nature of the aromatic rings, but also on the location of these heterocycles in the system [4]. Our research group has recently published experimental and theoretical results concerning the auxiliary donor/acceptor effect of electron rich and electron deficient heterocycles on push-pull thienylpyrrole π–conjugated systems. We have found that the position of the acceptor

groups such as dicyanovinyl or electron-deficient heterocycles (*e.g.* benzothiazole or benzimidazole), on the thienylpyrrolyl system have a clear influence on the NLO, spectroscopic (singlet and triplet state) and the photophysical properties in solution (at room and low temperature) [5].

The arylazo derivatives of the "pseudo-stilbene" type are characterized by a strong asymmetric electron distribution, which results from being substituted at the 4 and 4′ positions with electron-donating and electron-withdrawing groups (called a 'push/pull' substitution pattern). These pseudo-stilbenes have a strong and broad absorption feature in the visible, indicative of a sizeable electric dipole moment, possess nonlinear optical properties (owing to the asymmetric electron distribution), and often have a superlative photo-switching response, making them strong candidates for a variety of applications and studies [6]. In this context, aryl and heteroaryl azo dyes are a versatile class of organic compounds that have recently attracted the interest of many research groups due to their diverse optical applications [7-8]. Particularly, (hetero)arylpyrrole azo dyes are promising candidates for non linear optical and photochromic applications [3k, 3m, 9-10].

The photochemical $E \rightarrow Z$ isomerization of aromatic azo dyes, in solution or incorporated in polymeric matrices, can be achieved through visible irradiation (λ within the broad azo absorption band) and since the *E*-isomer is more stable then the *Z*-isomer once the irradiation source is turned off, the later is thermally reconverted back to the initial *E* form (Scheme 1). This conversion is accompanied by a change in the maximum absorption wavelength, since the *Z*-isomer absorbs at shorter wavelengths, the absorption peak being typically shift by 50 to 70 nm [11].

<Scheme 1>

Therefore, visible light promotes a $E \rightarrow Z$ conversion leading to a decrease of the absorption at the λ_{max} of the *E*-isomer and when the irradiation is ceased an absorption increase is observed due to the thermal back reaction $Z \rightarrow E$ whose rate constants can be calculated.

Under continuous visible irradiation conditions, the decrease in the absorbance at the λ_{max} of the *E* isomer is inversely related to the kinetic rate of the colouration process ($Z \rightarrow E$). Consequently, in similar systems, an increase in thermal colouration kinetics leads to lower absorbance variations.

Apart from a few recent reports [3k,3m,12] very little experimental work has been focused on the use of pyrroles or thienylpyrroles as building blocks for the synthesis of novel azo dyes for NLO and photochromic applications. Recently our group has been interested in the synthesis of new heterocyclic azo dyes prepared through azo coupling reaction using, for the first time, thienylpyrrole derivatives [13a-b], 5-alkoxy-2,2´-bithiophene moieties [14], 5-*N*,*N*-dialkylamino-2,2´-bithiophenes [15a] and aryldiazonium salts as coupling components. Moreover, the characterization of the thermal, nonlinear optical and photochromic properties of the novel azo dyes proved that they could be used as efficient and thermally stable solvatochromic probes, nonlinear optical [13a-b,14,15a] and photochromic materials [13c,15b].

Before our recent photochromic studies on azo dyes bearing thienylpyrrole [13c] and bithiophene [15b] systems, only a few reports concerning the photochromic properties of heterocyclic azo dyes were found in the literature [15c-e]. In our earlier studies, we have showed that, the kinetics of the azo isomerization reaction and the amplitude of the absorption variation are strongly dependent on the nature of the heterocyclic system (thienylpyrrole or bithiophene) and also on the position of the azo linkage on the bithiophene moiety. While aryldiazene thienylpirroles [13c] exhibit thermal $Z \rightarrow E$ isomerization rates around 0.30 s^{-1}, aryldiazene bithiophenes showed significantly slower rates (0.01-0.04 s^{-1}) indicating more stable *Z*-isomers [15b].

Given our previous results with the above mentioned azo dyes [13-14, 15a-b] and also other previous studies [3k,3m,12] we envisaged the use of a heterocycle that has never been considered for NLO applications in combination of conjugated 1-substituted pyrrole and 1-(alkyl)arylthienylpyrroles azo dyes. This synthetic strategy was employed having in mind the increase of the acceptor strength of the diazene moiety replacing the aryl ring, used earlier in the acceptor end [13a-b], by an electron-deficient heteroaromatic molecule having reduced aromaticity and electron-acceptor electronic character such as the thiazole heterocycle [3e,3f,4a-c].Using this heterocycle we sought to improve the intramolecular electronic delocalisation, leading to an enhancement of the second order hyperpolarizability β and photochromic properties of the new chromophores.

In this paper we report a systematic study of two series of organic chromophores consisting of newly synthesized thienylpyrrole **5-7** and pyrrole azo dyes **9-10**. The design and the synthesis

of these chromophores were based on different combination of electron-withdrawing groups, aryl or thiazole, linked to the pyrrole or thienylpyrrole strong π-electron donor moieties through an azo bridge. Their solvatochromic, electrochemical, nonlinear optical and photochromic properties along with the thermal stability have been investigated to better understand the influence of electron-accepting, electron-donor groups and π-conjugated heterocyclic bridges on the electronic and optical properties related to the ICT characteristics of the D-π-A dyes.

2. Results and discussion

2.1. Synthesis

We have recently reported the synthesis of thienylpyrroles **1** through the combination of Friedel-Crafts and Lawesson reactions [16]. These compounds have proved to be versatile substrates in azo coupling reactions, allowing the preparation of novel donor-acceptor substituted thienylpyrrole phenyldiazenes [13a-b].

The synthesis of thienylpyrrole **5-7** and pyrrole azo dyes **9-10** is outlined in Schemes 2-3. Thiazolyl and aryl amines were diazotized using $NaNO_2$ in HCl at 0 – 5 ^oC and the coupling reaction of (hetero)aryldiazonium salts **2-4**, with 1-alkyl(aryl)-2-(2´-thienyl)pyrroles **1**, in acetonitrile/acetic acid at 0 ºC, gave rise to the formation of the corresponding heterocyclic azo derivatives **5a-f**, **6b**, **7a**, **9b** and **10a-c** (Schemes 2-3). The azo coupling reaction was accomplished selectively at the 2-position [17] of the pyrrole ring to give thienylpyrroles **5a-f**, **6b** and **7a** in good yields (67-89%). These results are consistent with the greater nucleophilicity of the pyrrole ring *versus* the thiophene ring as has been shown earlier in the case of azo coupling, formylation and tricyanovinylation reactions of thienylpyrroles [12,13a-b,16b,18]. As expected, higher yields (77-89%) were obtained in the synthesis of thienylpyrrole azo dyes **5b-c** and **5e-f** bearing aryl groups substituted on 4- or 2,4- position(s) by electron donating groups when compared with propyl derivative **5a** (47%).

<Scheme 2>

<Scheme 3>

On the other hand, when compared to the yield of dye **10a** (85%), which was obtained from the unsubstituted aryldiazonium salt, the synthesis of pyrrole azo dyes **10** was achieved in higher yields for compounds **10b** (94%) and **10c** (95%) which were prepared through azo coupling using diazonium cations substituted by withdrawing groups (CN, NO_2) in the 4-position of the aryl ring (Scheme 3). These results follow from the fact that the azo coupling is an aromatic electrophilic substitution, therefore electron donor substituents on the pyrrole ring (R_1) and/or electron withdrawing groups (R_2) on the aryldiazonium salt should facilitate the reaction.

Another comparison could also be made having in mind the results previously obtained by us in the synthesis of thienylpyrrolyl aryldiazenes. In this case the introduction of the thiophene ring in position 2 of the pyrrole heterocycle leads to lower yields for thienylpyrroles **11b-c** (81-84%) [13a-b] compared to pyrroles **10b-c** (94-95%).

Thienylpyrrole azo dye **7a** was synthesized in order to compare the difference of the electronic and optical properties when a phenylazo moiety is substituted by an azothiazole system (*e.g.* **5a**) and pyrrole azo dyes **9b** and **10a-c** were synthesized in order to compare the effect of the π-conjugated bridge/donor auxiliary effect of the thiophene heterocycle on the electro optical properties of azothiazole thienylpyrrole (*e.g.* **5b**) and arylazo thienylpyrroles **11b-c** (Figure 1) [13a-b].

<Figure 1>

The structures of azo dyes bearing thienylpyrrole **5-7** or pyrrole conjugated systems **9-10** were unambiguously confirmed by their analytical and spectral data.

In the ^{1}H NMR spectra of azo thienylpyrrole derivatives **5a-f** and **6b** functionalized with a thiazolyldiazene moiety on the 2-position of the pyrrole ring two doubles at about 7.01-7.15 and 6.77-7.17 ppm were detected with coupling constants of 4.4-4.8 Hz indicating the presence of two adjacent protons (3´-H and 4´-H) at the corresponding pyrrole moiety. In the ^{1}H NMR spectrum of derivative **6b** bearing a 5-methyl-thiazole moiety two signals at 2.43 and 7.54 ppm were detected. Both signals appear as doublets with a coupling constant of 0.8 Hz. These signals were attributed respectively, to the methyl group attached to C5 and to the 4-H, in the thiazole moiety. In all the ^{1}H NMR spectra of thienylpyrrole azo dyes **5a-f** and **6b** three signals at about 7.05-7.08 (multiplet) 7.18-7.52 (double doublet), and 7.46-7.72 (double

doublet) were detected and were attributed respectively, to the 4´´, 3´´ and 5´´-H protons in the thiophene ring.

The ^{1}HNMR spectra confirm also a significant CT from the pyrrole or thienylpyrrole moieties to the hetero(aryl)azo groups and a high polarizability of the whole donor-acceptor derivatives. Therefore, the chemical shifts of azo dyes **10b-c** bearing stronger acceptor groups on the diazene moiety, exhibit signals that are downfield relative to the unsubstituted derivative **10a** indicating CT from the donor to the acceptor. The effect of the substitution of a phenyl group to the acceptor end for dye **7a** by a thiazole heterocycle (*e.g.* **5a**) is also noteworthy. All the protons of the thienylpyrrole **5a** (3´-H and 4´-H, and 3´´, 4´´and 5´´-H) were shifted to higher chemical shifts (*e.g.* 4´-H and 3´-H δ = 6.77 and 7.01 ppm respectively) when compared to the corresponding phenyldiazene azo dye **7a** (*e.g.* 4´-H and 3´-H δ = 6.58 and 6.88 ppm respectively) thus indicating a decrease of the electron density due to the stronger acceptor ability of the thiazole ring, allowing a more efficient charge transfer from the donor to the acceptor group. On the other hand stronger donor groups substituted on position 1 of the pyrrole ring of thienylpyrrole azo dyes leads to highfield signals thus again demonstrating the easy of electron communication within the whole heterocyclic system.

2.2. UV-visible study of thienylpyrrole 5, 6-7 and for pyrrole azo dyes 9-10

All compounds were soluble in common organic solvents, such as diethyl ether, ethanol, dioxane and DMSO. The absorption spectra data of azo dyes **5**, **6-7** and **9-10** in these solvents are summarized in Table 1. They show an intense lowest energy charge-transfer absorption band in the UV-vis region. The position of this band was strongly influenced by the structure of the compounds, for example by the type of π-conjugated bridge, by the substitution pattern in the donor and the acceptor moieties and also by the electronic nature of the acceptor moiety. The absorption maxima (λ_{max}) of the thienylpyrrole azo dyes **5**, **6-7** in dioxane are located at the range of 419 to 498 nm as opposed to the range of 386 to 419 nm for pyrrole azo dyes **9-10**. Dramatic differences in energy occur upon thiazolylazo or arylazo substitution of thienylpyrroles **1** and pyrrole **8**. For example, the absorption maxima, in ethanol for thienylpyrrole **1c** (λ_{max} = 286.5 nm) [13a] is shifted 219.5 nm upon thiazolylazo substitution (thienylpyrrole azo dye **5c**, λ_{max} = 506.0 nm) (Table 1).

As observed for other heterocyclic azo dyes, a bathochromic shift in the UV-Vis. spectra is observed when stronger donor and/or acceptor groups are linked to the heterocyclic system [13a-b,14a-b,15a,19]. Therefore, substitution of an arylazo system (*e.g.* **7a**) for a thiazolyl azo moiety (*e.g.* **5a**) leads to a red shift of 67 nm from 419 nm (*e.g.* **7a**) to 486 nm for thiazole azo dye **5a**. Due to the electron density deficiency on the ring C atoms, the thiazole heterocycle acts as an electron-withdrawing group and also as an auxiliary acceptor; in fact it is a stronger acceptor group than the phenyl ring [3e-f,4].
The ICT bands of pyrrole azo dyes **10b-c** in dioxane solutions are also red-shifted by 18 nm for **10b** (R_2 = CN, λ_{max} = 404 nm) and 31 nm for **10c** (R_2 = NO_2, λ_{max} = 417 nm) compared to the ICT band of the unsubstituted derivative **10a** (R_2 = H, λ_{max} = 386 nm) indicating that, the electron-accepting abilities of *p*-substituted phenyl groups increase, as expected, in the order **10a** < **10b** < **10c**.

On the other hand the electron-donor ability of the substituent on the pyrrole nitrogen atom has a smaller impact on the UV-vis spectra of thienylpyrrole azo dyes **5a-f**. For instance, the absorption maxima of compounds **5a** and **5c** were shifted from 486 nm (**5a**) to 497 nm (**5c**).

As anticipated, the introduction of a thiophene ring induces a significant bathochromic shift on the UV-vis spectra of azo thienylpyrrole **5b** and thienylpyrrole derivatives **11b-c [**13a-b] compared to their pyrrole counterparts **9b** and **10b-c** respectively. The difference in λ_{max} values between compound **5b** and **9b** in dioxane is 74 nm while for compounds **11b-c** the difference is even larger (69-80 nm) when compared to the pyrroles **10b-c** as a result of a more extensive electron delocalization (Table 1). These observations confirm previously obtained results, namely that the incorporation of thiophene units in push-pull compounds enhances their charge-transfer properties, and can be explained considering the bathochromic effect of sulphur, the partial decrease of aromatic character of the thiophene heterocycle and also the increase of the π-overlap between the thiophene and the pyrrole units [20].

2.3. Solvatochromic study of azo dyes 5-7 and 9-10

Previous studies have demonstrated that donor-acceptor substituted thienylpyrroles exhibit a positive solvatochromism [5,13a-b]. In order to investigate whether thienylpyrroles **5-7** and pyrroles **9-10** exhibit the same behavior, we carried out a study of the absorption spectra for

all compounds in four selected solvents of different solvatation character (diethyl ether, ethanol, dioxane and DMSO). The wavelength maxima λ_{max} of compounds **5-7** and **9-10** are listed in Table 1 and were compared with the π^* values for each solvent, as determined by Kamlet and Taft [21]

Moderate to large positive solvatochromism ($\Delta\nu_{max}$ = 884-1058 cm^{-1}) was observed moving from diethyl ether to DMSO solutions for thiazolyl diazene derivatives **5a-f** and **6b**. On the other hand pyrrole azo dyes **10** exhibit smaller positive solvatochromism ($\Delta\nu_{max}$ = 400-882 cm^{-1}) compared to their thienylpyrrole counterparts [13a].

In agreement with other solvatochromic studies for heteroaryl-azo dyes, the increase of the electron-withdrawing strength of the substituent of the diazo component and/or the increase of the electron-donating strength of the coupling moiety was found to cause pronounced bathochromism [13a,14,15a,19]. Therefore, the pyrrole azo dyes with stronger acceptor groups on the azophenyl moiety (**10b**-**c**) and the thienylpyrroles bearing stronger donor groups substituted on position 1 of the pyrrole ring (*e.g.* **5c**) display a comparatively larger solvatochromism when compared to the unsubstituted compound **10a** and with the alkyl thienylpyrrole derivative **5a**, respectively. The same trend was observed when a diazenephenyl moiety (**7a**, $\Delta\nu_{max}$ = 739 cm^{-1}) was substituted by a thiazolyldiazene system (**5a**, $\Delta\nu_{max}$ = 884 cm^{-1}), due to the electron deficient nature of the thiazole heterocycle.

These sizable solvatochromic responses are indicative of highly polarizable π-conjugated structures. These features are key factors in designing efficient second-order NLO-chromophores [22]. Therefore, the UV-vis optical data suggest that the chromophores **5a-f** and **6b** will have greater hyperpolarizabilities than the pyrroles **10**.

<Table 1>

2.4. Electrochemical properties of compounds 5-7 and 9-10

The redox properties of thienylpyrroles (**5a-f**, **6b** and **7a**) and pyrrole azo dyes (**9b**, **10a**-**c**) were studied by cyclic voltammetry in DMF containing tetrabutylammonium tetrafluoroborate (0.10 M) as the supporting electrolyte. Table 2 lists the reduction and oxidation onsets and the electrochemical band gap values.

Upon azo coupling reactions, the azo dyes bearing thienylpyrrole **5** and pyrrole systems **9**-**10** display oxidations at more positive potentials as a consequence of the destabilizing effect of

the electron-withdrawing groups (thiazole or functionalized phenyl rings) on the diazene moiety. For example pyrrole azo dye **9b** displays an oxidation at E_{pa} = 0.69 V, corresponding to a negative shift of 0.17 eV with respect to the unsubstituted pyrrole **8**.

<Table 2>

All thienylpyrrole azo dyes bearing a thiazole acceptor group (**5a-f** and **6b**) exhibit two monoelectronic reversible reductions and one oxidation process (Figure 2). On the other hand, the thienylpyrrole azo dye **7a** and the pyrrole azo dyes with aryl end groups **10a-b** exhibit, in cathodic scans only one reversible reduction process. The dye **10c** exhibits a similar first reduction process while the second reduction process is assigned to the reduction of the nitro group. The one-electron stoichiometry for these reduction processes was ascertained by comparing the current heights with known one-electron redox processes under identical conditions [13a-b,23-24]. For all compounds, the first process was associated with the reversible reduction of the (hetero)aromatic azo moiety. For all azo derivatives it was also observed that the reduction potential values are only slightly influenced by the substituent on the nitrogen atom of the pyrrole ring or by the introduction of a thiophene ring on the pyrrole system. Therefore, the difference between the reduction potentials obtained for thienylpyrroles and the corresponding pyrrole derivatives are between 0.03 and 0.05 V.

<Figure 2>

All thienylpyrrole and pyrrole azo dyes undergo oxidation due to the absence of substituents in 5´´ position of the thiophene (**5a-f**, **6b** and **7a**) or in 5´ position of the pyrrole (**9b** and **10a-c**) groups. Dimerization via the electrogenerated radical cations has been shown to usually occur at such positions [25].

The data obtained for the process of the oxidation illustrate that there is a prominent electrochemical distinction between the compounds depending on the type of donor and acceptor groups (Table 2). Contrary to the reduction process, a comparison of the oxidation potentials obtained for thienylpyrroles and the corresponding pyrrole azo dyes bearing the same group substituted on position 1, of the pyrrole ring, showed a remarkable difference in these values due to the effect of the length and the different electronic nature of the π-conjugated bridge (*e.g.* **5b**, E_{pa} = 0.57 V and **9b** E_{pa} = 0.69 V). The observed shifts are a direct

consequence of the extent of donor-acceptor coupling [5a,9f,13a]. The same trend was observed for pyrroles **10b-c** compared to thienylpyrroles **11b-c** [11a]. Since the oxidation potential is directly related to the ionization potential or the tendency of losing electron, it is expected that thienylpyrrole chromophores have a more efficient ICT from the donor to the acceptor compared to their pyrrole countarparts.

It was also observed, that the decrease of the acceptor group ability on the aryldiazene moiety of pyrroles **10a-c** results in a negative shift of the oxidation potential (*e.g.* **10a** E_{pa} = 0.76 V and **10c** E_{pa} = 0.81 V). On the other hand, compound **7a** with an azophenyl moiety, exhibits only a slight cathodic shift due to the weaker withdrawing acceptor strength of the phenyl ring compared to the thiazole heterocycle.

Electrochemical band gaps were calculated as described previously from the potentials of the anodic (oxidation of the thienylpyrrole or pyrrole groups) and cathodic processes [20d,26].

The analysis of the electrochemical data for compounds **5-7** and **9-10** showed that several factors influence the electronic nature of the π-conjugated systems leading to a decrease of the band gap values:
i) the strength of the donor group linked to position 1 of the pyrrole ring (*e.g.* **5a**, 2.10 eV; **5c**, 2.06 eV);
ii) the strength and electronic nature of the acceptor group linked to the diazene system (*e.g.* **10a**, 2.66 eV; **10c**, 2.11 eV or **7a**, 2.51 eV; **5a**, 2.10 eV);
iii) the length of the π-conjugated bridge (*e.g.* **9b**, 2.22 eV; **5b**, 2.07 eV).

The results clearly show that there is a much more efficient coupling between the thienylpyrrole and pyrrole systems and the thiazole acceptor as compared to the aryl acceptor groups. The efficient donor-acceptor conjugation leads to a raising and lowering of the HOMO and LUMO levels, respectively. In contrast a weaker donor-acceptor coupling provokes the opposite effect: the lowering of the HOMO level and the a raising of the LUMO level. The measured HOMO/LUMO values and how they are influenced by the electronic groups are consistent with the spectroscopic measurements.

2.5. Non-linear optical properties and thermal stability of thienylpyrrole 5-7 and pyrrole azo dyes 9-10

We have used the hyper-Rayleigh scattering (HRS) method [27] to measure the first hyperpolarizability β of thienylpyrrole **5-7** and pyrrole azo dyes **9-10** using the 1064 nm fundamental wavelength of a laser laser beam. Dioxane was used as the solvent, and the β values were measured against a reference solution of *p*-nitroaniline (*p*NA) [28] in order to obtain quantitative values, while care was taken to properly account for possible fluorescence of the dyes (see experimental section for more details). The static hyperpolarisability β_0 values were calculated using a very simple two-level model neglecting damping. They are therefore only indicative and should be treated with caution (Table 3).

From Table 3 it can be seen that the NLO chromophores **5a-f**, **6b** and **11b-c** exhibit moderate to good molecular nonlinearities as their β values are 7-25 times higher that of the well known *p*NA molecule for an incident laser wavelength of 1064 nm (the corresponding β_0 values are 2 to 7 times higher than that of *p*NA).

Earlier, some of us reported the synthesis, solvatochromic and electrochemical properties of aryldiazene thienylpyrrole derivatives **11b-c** [13a]. The first order hyperpolarizabilities of these compounds were now also studied in order to compare their values with those of the pyrrole azo dyes **10b-c**. The introduction of a thiophene ring on the azo dyes **11b-c** leads to higher β values (**11b-c**; β = 345 – 415 x 10^{-30} esu) when compared to their pyrrole counterparts (**10b-c**; β = 84 – 128 x 10^{-30} esu). As expected, the same trend was observed for the thienylpyrrole thiazolylazo dye **5b**, (β = 156 x 10^{-30} esu) when compared to the corresponding thiazolylazo pyrrole derivative **9b** (β = 80 x 10^{-30} esu). We attribute this as being due to the more extensive electron delocalization.

Moreover, compounds functionalized with 2,4-dimethoxyphenyl- (**5c**), 4-fluorophenyl- (**5e**) and 4-bromophenyl- (**5f**) groups, on position 1 of the pyrrole ring exhibit larger nonlinearities as compared to the other thienylpyrrole azo dyes. It is also noteworthy the effect of the functionalization of the thiazole ring with a methyl group (*e.g.* **6b**), which increases the β values from 156 x 10^{-30} esu for compound **5b** to 274 x 10^{-30} esu for **6b**.

From Table 3 it can be seen that the β values of pyrrole azo dyes **10b** (β = 84 x 10^{-30} esu) and **10c** (β = 128 x 10^{-30} esu) are strongly influenced by the strength of the acceptor group (CN < NO_2) substituted on the arylazo moiety. As expected, the same trend (H < CN < NO_2) was observed for the corresponding thienylpyrroles derivatives **7a**, **11b** and **11c**. Indeed, the β values increased from 95 x 10^{-30} esu for **7a** (R = H) to 345 x 10^{-30} esu for **11b (**R = CN) reaching the higher value of 415 x 10^{-30} esu for **11c** (R = NO_2).

The comparison of the second order hyperpolarizabilities for compounds **5a** and **7a** also showed that the electron-deficient thiazole heterocycle has a larger acceptor strength than the phenyl ring, as the β value of the thiazolyldiazene **5b** (β = 164 x 10^{-30} esu) was almost two times larger than the corresponding value for the phenyldiazene **7a** (β = 95 x 10^{-30} esu). Due to the deficiency of electron density on the ring C atoms, the thiazole heterocycle acts as electron-withdrawing group and also as an auxiliary acceptor. Furthermore, the large electronegativity and lone electron pairs of S and N atoms in thiazole together with the extension of the conjugation length of the π-electron bridge also lead to an increase in molecular hyperpolarizability, showing that thiazole derivatives are a good choice for NLO applications [3e-f,3i-3j,4a-c].

The thermal stabilities of the resulting azo dyes **5-7** and **10-11** were evaluated by thermogravimetric analysis (TGA) under a nitrogen atmosphere, measured at a heating rate of 20 ºC min^{-1}. As shown in Table 3 all compounds exhibit good to excellent thermal stability with decomposition temperatures varying from 206 to 288 ºC for thienylpyrrole azo dyes **5a-f**, **6b** and **11b-c**. Pyrrole derivatives **11b-c** decompose between 216-227 ºC, while thienylpyrrole azo dyes (*e.g.* **11b-c**) showed an improved thermal stability by *ca* 59-62 ºC. In addition, the electronic nature of the substitutents on position 1 of the thienylpyrrole azo dyes **5a-f** have some influence on their thermal stability being higher for R_1 = 2,4-diOMePh, T_d = 273 ºC, (Table 3).

<Table 3>

<Figure 3>

2.6. Photochromic properties of thienylpyrrole 5-7 and pyrrole azo dyes 9-10

The photochromic properties of azo dyes **5a-f**, **6b**, **7a** and pyrrole derivatives **9b** and **10a-c** were studied in 2.0 $\times 10^{-5}$ M acetone solutions by irradiating them with visible light (λ>420 nm) from a 150 W ozone free xenon lamp equipped with a water filter and a long-pass filter Schott GG 420 at 20 ºC and simultaneously monitoring absorbance of the solutions at their corresponding wavelength of maximum absorption. The irradiation of the thienylpyrrole azo dye **5a-f**, **6b**, **7a** solutions led to a very fast and pronounced decrease of the maximum absorbance at longer wavelengths and, at the same time, an increase in the band located at

380-400 nm, indicating the transformation of the more stable *E*-isomer to the *Z*-isomer. The change in the visible spectra of dye **5a** is depicted in Figure 4. When the irradiation was stopped the inverse situation was observed, the band at 380 nm decreased and the band at 487 nm increased.

<Figure 4>

The absorbance variation observed under visible irradiation of diazenethiazolyl thienylpyrroles **5a-f** varies from 0.10 to 0.15 absorbance units corresponding to a loss of 20–22% of the initial absorbance. The procedure was subsequently repeated and the behavior was fully reproducible indicating that under these experimental conditions no noticeable degradation occurred. For methylthiazole azo dye **6b** the decrease in the absorption was considerably lower (7.8%) while for the diazenephenyl azo dye **7a** and pyrrole azo dyes **9b**, **10a-c** and **11b** the absorption variations were significantly higher (50-66%) (Table 4).

For the new thiazole azo dyes **5a-f** and **6b** the decrease in the absorbance, due to the $E \rightarrow Z$ transformation, was very fast and in less than 1.5 s a photostationary equilibrium was attained. For pyrrole azo dyes **10a-c** the decolouration rate was much slower and the photostationary equilibrium was attained only after 35-90 s of irradiation. When the irradiation ceased the system returned to its initial highly coloured state with different rates depending on the dye structure. The kinetics of the decolouration and colouration process of dyes **5a** and **7a** are shown in Figure 5.

<Table 4>

<Figure 5>

The kinetics of the thermal Z→E back reaction (colouration, in the dark, at 20ºC) for the thiazolyl thienylpyrrole azo dyes **5a-f** and **6b** were very fast (k_{Δ}=1.4-0.62 s^{-1}) but effectively independent of the nature of the substituent present on the pyrrole ring ($t_{1/2}$ (Z-isomer) between 0.5 and 1.1 s). The high thermal $Z \rightarrow E$ reaction rate observed with these compounds and the limited magnetic stirring of the solution, leads to a considerable oscillation of the absorbance at the photostationary equilibrium (Figure 5, compound **5a**), which is less significant for slower systems like compound **7a** (Figure 5).

Pyrrole azo dyes **10a-c** showed very slow kinetics of the thermal back *Z*→*E* isomerization ($9.5x10^{-3}$ to $5.2x10^{-4}$ s^{-1}), indicating a relatively high stability of the Z-isomer ($t_{1/2}$ = 70 - 1330 s). For these compounds the switching rates between the two isomers are quite slow.

From the comparative analysis of these thienylpyrrole and pyrrole azo dyes we can conclude that the substitution of the thiazole ring by a phenyl ring [comparison between compounds **5a** ($t_{1/2}$ = 0.5 s) and **7a** ($t_{1/2}$ = 20 s)] leads to a more stable Z species as indicated by the significant reduction of the thermal back reaction. The removal of the thiophene ring on diazenethiazolyl dyes [comparison between compounds **5b** ($t_{1/2}$= 1.1 s) and **9b** ($t_{1/2}$ = 36 s)] has a similar effect. The same trend was also observed for diazenearyl pyrrole **10c** when compared to the corresponding thienylpyrrole **11c**.
The introduction of substituents with increased acceptor strength on the diazenearyl moiety of pyrrole dyes **10a-c**, has a strong effect on the kinetics of the thermal back isomerization. Therefore, the presence of a stronger acceptor group such as nitro leads clearly to faster kinetics (*e.g.* **10a**, R = H, $t_{1/2}$ = 1330 s; **10c**, R = NO_2, $t_{1/2}$ = 70 s). This effect, already observed with diazenearyl thienylpyrroles [11c], can also be seen by comparing compounds **7a** (R = H, $t_{1/2}$ = 20 s) and **11c** [11c] (R = NO_2, $t_{1/2}$ = 2.1 s).

Overall within this set of compounds the thienylpyrrole bearing diazenethiazolyl moieties **5a-f** and **6b** showed the best photochromic behaviour: fast decouloration promoted by visible light stimulus (1.5 s) with a relatively high absorbance variation (20%) and very fast thermal back colouration (2-3 s) to the initial state, thus performing fast reproducible cycles.

3. Conclusions

We have synthesized two new series of azo dyes, based on the 1-alkyl(aryl)thienylpyrrole and 1-(4-methoxyphenyl)pyrrole as donors and simultaneously as π-conjugated bridges, and diazenearyl and diazenethiazolyl acceptor moieties. Extensive characterization of the optical (linear and nonlinear) electrochemical, thermal and photochromic properties was carried out. The new compounds were synthesized from easily available thienylpyrroles **1** and low cost, commercially available (hetero)aromatic anilines and pyrrole **8**. Simple work-up procedures produce moderate to excellent yields of these derivatives.

Despite the large number of donor-acceptor systems showing NLO and photochromic properties reported in the literature, the present concept of combining the donor properties of electron-rich pyrrole and thienylpyrrole heterocyclic systems with the electron deficient thiazole moiety in azo dye derivatives has not, to the best of our knowledge, been previously communicated in the literature.

This multidisciplinary study shows that the electronic nature of the withdrawing group substituted on the azo moiety and the type of π-conjugated system (pyrrole or thienylpyrrole) of the different synthesized azo dyes, has a remarkable influence on the electronic, optical (linear and nonlinear optical), photochromic and thermal properties of these donor-acceptor systems. The NLO and the photochromic properties of these heteroaromatic azo dyes, in particular the kinetics of the back isomerisation, can be modulated using thienylpyrrole sytems instead of pyrrole derivatives and/or through the introduction of different diazene (hetero)aryl moieties. Moreover, these new derivatives bearing thiazole moieties exhibit improved photochromic properties compared to the previously described diazenearyl azo dyes. In conclusion, the thienylpyrrole derivatives **5a-f** and **6b**, are endowed with good second-order molecular NLO activity, good thermal stabilities and excellent photochromic properties making them interesting candidates as prospective second-order NLO materials, as novel molecular switches or memory and recording devices.

4. Experimental

4.1. Materials

Aniline, 4-cyanoaniline, 4-nitroaniline, 2-aminothiazole, 2-amino-5-methylthiazole used as precursors for the synthesis of aryldiazonium salts **2-4** and 1-(4´-methoxyphenyl)pyrrole, were purchased from Aldrich and Fluka and used as received.

The synthesis of 1-alkyl-thienylpyrrole **5a [**16b] and 1-aryl-thienylpyrroles **5b-f [**16a] was described elsewhere. TLC analyses were carried out on 0.25 mm thick precoated silica plates (Merck Fertigplatten Kieselgel $60F_{254}$) and spots were visualised under UV light. Chromatography on silica gel was carried out on Merck Kieselgel (230-240 mesh).

4.2. Synthesis

4.2.1. General procedure for the azo coupling of thienylpyrroles 1 with thiazolyl-diazonium salts 2-3 and aryl-diazonium salt 4a to afford azo dyes 5a-f, 6b and 7a

4.2.1.1. Diazotisation of 2-aminothiazole, 2-amino-5-methylthiazole and aniline

Primary aromatic and heteroaromatic amines (1.0 mmol) were dissolved in HCl 6N (1 mL) at 0 - 5 ºC. A mixture of $NaNO_2$ (1.0 mmol) in water (2 mL) was slowly added to the well-stirred mixture of the thiazole solution at 0 - 5 ºC. The reaction mixture was stirred for 10 min.

4.2.1.2. Coupling reaction with thienylpyrroles 1

The diazonium salt solution previously prepared (1.0 mmol) was added dropwise to the solution of thienylpyrroles **1** (0.52 mmol) in acetonitrile (10 mL) and 2-3 drops of acetic acid. The combined solution was maintained at 0 ºC for 1 to 2 h while stirred and then diluted with chloroform (20 mL), washed with water and dried with anhydrous $MgSO_4$. The dried solution was evaporated and the remaining azo dyes purified by column chromatography on silica with dichoromethane/*n*-hexane as eluent.

1-(1-(Propyl-5-(thiophen-2-yl)-1*H*-pyrrol-2-yl)-2-(thiazol-2-yl)diazene (**5a).** Dark red solid (74 mg, 47%). Mp 68-69 ºC. ^{1}H NMR (Acetone-d_6) δ 0.98 (t, *J*=7.6 Hz, 3H, CH_3), 1.85-1.94 (m, 2H, CH_2), 4.54 (t, *J*=7.6 Hz, 2H, NCH_2), 6.77 (d, 1H, *J*=4.4 Hz, 4'-H), 7.01 (d, 1H, *J*=4.4 Hz, 3'-H), 7.27-7.29 (m, 1H, 4''-H), 7.52 (dd, *J* = 4.0 and 1.2 Hz, 3''-H), 7.54 (d, 1H, *J*=3.6 Hz, 5-H), 7.72 (dd, 1H, *J*=5.2 and 1.2 Hz, 5''-H), 7.92 (d, 1H, *J*=3.6 Hz, 4-H). ^{13}C NMR (Acetone-d_6) δ 11.4, 25.4, 46.3, 105.0, 115.2, 120.0, 128.2, 128.4, 129.1, 133.3, 136.5, 144.2, 147.5, 179.9. λ_{max}(Dioxane)/nm 486 (ε/dm^3 mol^{-1} cm^{-1} 25,400). IR (Nujol) ν/ cm^{-1} 3075, 1619, 1504, 1341, 1297, 1214, 1162, 1135, 1017, 874, 851, 775, 721, 621. MS (microTOF) *m/z* (%) = 303 ([M+H] $^+$, 100), 207 (2). HMRS: *m/z* (MicroTOF) for $C_{14}H_{15}N_4S_2$; calcd 303.0738; found: 303.0733.

1-(1-(4-Methoxyphenyl)-5-(thiophen-2-yl)-1*H*-pyrrol-2-yl)-2-(thiazol-2-yl)diazene (**5b).** Violet solid (146 mg, 77%). Mp 124-126 ºC. ^{1}H NMR (Acetone-d_6) δ 4.00 (s, 3H, OCH_3), 7.00 (d, 1H, *J*=4.4 Hz, 4'-H), 7.04-7.07 (m, 1H, 4''-H), 7.14 (d, 1H, *J*=4.4 Hz, 3'-H), 7.17-7.18 (m, 3H, 3''-H, 3'''-H and 5'''-H), 7.40-7.42 (m, 3H, 5-H, 2'''-H and 6'''-H), 7.49 (dd, 1H, *J*=4.8 and 1.2 Hz, 5''-H), 7.85 (d, 1H, 4-H, *J*=3.2 Hz). ^{13}C NMR (Acetone-d_6) δ 55.9,

104.8, 113.9, 115.0, 120.2, 127.8, 128.3, 129.6, 131.4, 133.7, 130.0, 144.1, 149.5, 161.3, 179.8. λ_{max}(Dioxane)/nm 493 (ε/dm^3 mol^{-1} cm^{-1} 25,830). IR (Nujol) ν/ cm^{-1} 2954, 1609, 1515, 1403, 1334, 1297, 1243, 1220, 1195, 1174, 1145, 1044, 1022, 1002, 877, 852, 772, 711, 614. MS (microTOF) *m/z* (%): 367 ([M+H]$^+$, 100), 303 (6), 221 (4), 207 (8). HMRS: *m/z* (MicroTOF) for $C_{18}H_{15}N_4OS_2$; calcd 367.0687; found: 367.0682.

1-(1-(2,4-Dimethoxyphenyl)-5-(thiophen-2-yl)-1*H*-pyrrol-2-yl)-2-(thiazol-2-yl)diazene (5c). Violet solid (171 mg, 83%). Mp 125-126 ºC. ^{1}H NMR (Acetone-d_6) δ 3.72 (s, 3H, OCH_3), 3.96 (s, 3H, OCH_3), 6.74 (dd, 1H, *J*=8.8 and *J*=2.8 Hz, 5'''-H), 6.84 (d, 1H, *J*=4.8 Hz, 3'-H), 7.05 (d, 1H, *J*=4.4 Hz, 3'''-H), 7.05-7.08 (m, 1H, 4''-H), 7.14 (d, 1H, *J*=4.8 Hz, 4'-H), 7.28 (dd, 1H, *J*=3.6 and *J*=1.2 Hz, 3''-H), 7.34 (d, 1H, *J*=8.8 Hz, 6'''-H), 7.36 (d, 1H, *J*=3.6 Hz, 5-H), 7.46 (dd, 1H, *J*=5.2 and *J*=1.2 Hz, 5''-H), 7.83 (d, 1H, *J*=3.6 Hz, 4-H). ^{13}C NMR (Acetone-d_6) δ 56.3, 56.0, 79.2, 100.2, 105.8, 113.6, 118.6, 119.8, 127.3, 128.1, 128.2, 132.2, 133.8, 138.5, 144.0, 148.9, 158.3, 163.1, 178.0. λ_{max}(Dioxane)/nm 497 (ε/dm^3 mol^{-1} cm^{-1} 21,960). IR (Nujol) ν/ cm^{-1} 2954, 1588, 1515, 1402, 1338, 1329, 1301, 1256, 1242, 1221, 1210, 1197, 1160, 1001, 878, 836, 791, 723. MS (microTOF) *m/z* (%): 397 ([M+H]$^+$, 100), 359 (2), 259 (2), 233 (4). HMRS: *m/z* (microTOF) for $C_{19}H_{17}N_4O_2S_2$; calcd 397.0793; found: 397.0787.

1-(1-(3,4,5-Trimethoxyphenyl)-5-(thiophen-2-yl)-1*H*-pyrrol-2-yl)-2-(thiazol-2-yl)diazene (5d). Violet solid (155 mg, 70%). Mp 182-184 ºC. ^{1}H NMR (Acetone-d_6) δ 3.85 (s, 6H, 2xOCH_3), 3.88 (s, 3H, OCH_3), 6.84 (br s, 2H, 2'''-H and 6'''-H), 7.02 (d, 1H, *J*=4.4 Hz, 3'-H), 7.07-7.10 (m, 1H, 4''-H), 7.15 (d, 1H, *J*=4.4 Hz, 4'-H), 7.21 (dd, 1H, *J*=4.0 and *J*=1.0 Hz, 3''-H), 7.42 (d, 1H, *J*=3.6 Hz, 5-H), 7.52 (dd, 1H, *J*=5.2 Hz, J=1.0 Hz, 5''-H), 7.83 (d, 1H, *J*=3.6 Hz, 4-H). ^{13}C NMR (Acetone-d_6) δ 56.8, 60.9, 104.6, 108.4, 113.9, 120.3, 128.0, 128.3, 128.4, 132.3, 133.5, 137.74, 140.1, 144.1, 149.1, 154.5, 179.9. λ_{max}(Dioxane)/nm 494 (ε/dm^3 mol^{-1} cm^{-1} 27,100). IR (Nujol) ν/ cm^{-1} 3115, 3101, 3075, 2956, 1748, 1598, 1535, 1505, 1485, 1423, 1407, 1365, 1343, 1315, 1284, 1242, 1222, 1193, 1185, 1167, 1143, 1123. MS (microTOF) *m/z* (%): 427 ([M+H]$^+$, 100), 233 (2). HMRS: *m/z* (MicroTOF) for $C_{20}H_{19}N_4O_3S_2$; calcd 427.0899; found: 427.0893.

1-(1-(4-Fluorophenyl)-5-(thiophen-2-yl)-1*H*-pyrrol-2-yl)-2-(thiazol-2-yl)diazene (5e). Violet solid (158 mg, 86%). Mp 120-124 ºC. ^{1}H NMR (Acetone-d_6) δ 7.02 (d, 1H, *J*=4.4 Hz, 4'-H), 7.06-7.09 (m, 1H, 4''-H), 7.16-7.17 (m, 3H, 3' and 3''-H and 5´´-H), 7.39-7.44 (m, 3H,

5-H, 3’’’-H and 5’’’-H), 7.53 (dd, 1H, *J*=4.8 and *J* =1.2 Hz, 5’’-H), 7.58 (dd, 2H, *J*=9.0 and *J*=5.2 Hz, 2’’’-H and 6’’’-H), 7.84 (d, 1H, *J*=3.2 Hz, 4-H). ^{13}C NMR (Acetone-d_6) δ 104.9, 114.2, 116.6 and 116.9 (d, *J*=23 Hz), 120.4, 128.1, 128.4, 132.5 and 132.6 (d, *J*=9 Hz), 133.4, 133.4, 133.4, 137.8, 144.2, 149.3, 162.6 and 165.1 (d, *J*=246 Hz), 179.7. λ_{max}(Dioxane)/nm 491 (ε/dm^3 mol^{-1} cm^{-1} 25,300). IR (Nujol) *v*/ cm^{-1} 1510, 1306, 1217, 1200, 1147, 1044, 968, 839. MS (microTOF) *m/z* (%): 355 ([M+H] $^+$, 100), 337 (4), 300 (3), 233 (2). HMRS: *m/z* (MicroTOF) for $C_{17}H_{12}FN_4S_2$; calcd 355.0487; found: 355.0482.

1-(1-(4-Bromophenyl)-5-(thiophen-2-yl)-1*H*-pyrrol-2-yl)-2-(thiazol-2-yl)diazene (5f). Violet solid (186 mg, 86%). Mp 172-174 ºC. ^{1}H NMR (Acetone-d_6) δ 7.00 (d, 1H, *J*=4.4 Hz, 3’-H), 7.07-7.10 (m, 1H, 4’’-H), 7.16 (m, 2H, 3’’-H and 5’-H), 7.45 (d, 1H, *J*=3.6 Hz, 5-H), 7.50 (d, 2H, *J*=8.8 Hz, 2’’’-H and 6’’’-H), 7.54 (dd, 1H, *J*=5.2 and J=1.2 Hz, 5’’-H), 7.83 (d, 2H, *J*=8.8 Hz, 3’’’-H and 5’’’-H), 7.88 (d, 1H, *J*=3.6 Hz, 4-H). ^{13}C NMR (Acetone-d_6) δ 105.0, 114.5, 120.5, 123.7, 128.2, 128.5, 132.4, 133.0, 133.2, 136.6, 137.5, 144.2, 149.1, 179.5. λ_{max}(Dioxane)/nm 489 (ε/dm^3 mol^{-1} cm^{-1} 31,840). IR (Nujol) *v*/ cm^{-1} 1736, 1402, 1340, 1302, 1218, 1212, 1194, 1169, 1141, 1043, 1022, 1004, 967, 897, 876, 850, 835, 768. MS (microTOF) *m/z* (%): 417 ([M+H]$^+$ ^{81}Br, 100), 415 ([M+H]$^+$ ^{79}Br, 97), 259 (8), 233 (13). HMRS: *m/z* (microTOF) for $C_{17}H_{12}{}^{81}BrN_4S_2$; calcd 416.9687; found: 416.9681.

1-(1-(4-Methoxyphenyl)-5-(thiophen-2-yl)-1*H*-pyrrol-2-yl)-2-(5-methylthiazol-2-yl)diazene (6b). Violet solid (176 mg, 89%). Mp 118-120 ºC. ^{1}H NMR (Acetone-d_6) δ 2.43 (d, 3H, *J*=0.8 Hz, 5-CH_3), 3.95 (s, 3H, OCH_3), 6.95 (d, 1H, *J*=4.8 Hz, 3’-H), 7.03-7.05 (m, 1H, 4’’-H), 7.07 (d, 1H, *J*=4.8 Hz, 4’-H), 7.12 (dd, 1H, *J*=3.6 and *J*=1.2 Hz, 3’’-H), 7.15 (d, 2H, *J*=8.8 Hz, 3’’’-H and 5’’’-H), 7.39 (d, 1H, *J*=8.8 Hz, 2’’’-H and 6’’’-H), 7.47 (dd, 1H, *J*=4.0 and *J*=1.2 Hz, 5’’-H), 7.54 (d, 1H, *J*=0.8 Hz, 4-H). ^{13}C NMR (Acetone-d_6) δ 12.6, 55.9, 104.1, 113.6, 115.0, 127.6, 128.0, 128.3, 129.7, 131.4, 133.8, 135.5, 137.4, 142.2, 149.5, 161.2, 177.6. λ_{max}(Dioxane)/nm 498 (ε/dm^3 mol^{-1} cm^{-1} 24,820). IR (Nujol) *v*/ cm^{-1} 2960, 1511, 1301, 1246, 1196, 1169, 1031, 966, 892, 835, 773, 722. MS (EI) *m/z* (%): 351 ([M+1]$^+$, 5), 350 ([M$^+$, 20), 270 (60), 253 (25), 121 (37) HMRS: *m/z* (EI) for $C_{19}H_{16}N_4S_2O$; calcd: 380.0766; found: 380.0770.

2-Phenyl-(1-(1-propyl-5-(thiophen-2-yl)-1*H*-pyrrol-2-yl)diazene (7a). Orange oil (102 mg, 67%). ^{1}H NMR ($CDCl_3$) δ 0.98 (t, *J*=7.6 Hz, 3H, CH_3), 1.85-1.94 (m, 2H, CH_2), 4.51 (t, *J*=7.6 Hz, 2H, NCH_2), 6.58 (d, 1H, *J*=4.4 Hz, 4’-H), 6.88 (d, 1H, *J*=4.4 Hz, 3’-H), 7.13-7.16 (m, 1H,

4'' -H), 7.24 (dd, *J*= 4.0 and *J*=1.2 Hz, 3''-H) 7.37-7.40 (m, 2H, 4-H and 5''-H), 7.48 (t, 2H, *J*= 7.2 Hz, 5-H) 7.85 (dd, 2H, *J*=5.2 and *J*=1.2 Hz, 5'''-H), 7.87 (dd, 2H, *J*=1.0 and *J*=7.2 Hz, 2''-H and 6''-H). ^{13}C NMR ($CDCl_3$) δ 11.4, 25.0, 45.6, 104.6, 115.2, 120.0, 128.2, 128.4, 129.1, 133.3, 136.5, 144.2, 147.5. λ_{max}(Dioxane)/nm 419 (ε/dm^3 mol^{-1} cm^{-1} 18,300). IR (Liquid film) ν/ cm^{-1} 2959, 1594, 1495, 1368, 1345, 1032, 846, 765, 694. MS (EI) *m/z* (%): 295 (M^+, 50), 203 (66), 162 (40), 121 (65). HMRS: *m/z* (EI) for $C_{17}H_{17}N_3S$; calcd: 295.1143; found: 295.1141.

4.2.2. General procedure [30] for the azo coupling of pyrrole 8 with diazonium salts 2 and 4a to afford azo dyes 9b and 10a

4.2.2.1. Diazotisation of aniline and 2-aminothiazole

To a suspension of the (hetero)aromatic amines (0.86 mmol) in water (2 mL) was added concentred HCl (2.5 mmol, 0.21 mL) until the mixture was homogeneous. The solution was cooled and kept at 0 - 5 ºC in a ice bath and a solution of $NaNO_2$ (0.89 mmol) in water (1 mL) was slowly added to the well-stirred mixture of the thiazole solution at 0 - 5 ºC. The reaction mixture was stirred during 20-30 min.

4.2.2.2. Coupling reaction with pyrrole 8

The diazonium salt solution previously prepared (0.86 mmol) was added dropwise to the solution of pyrrole **8** (1 mmol) and pyridine (1mL, 1.25 mmol) in methanol (20 mL). The solution was stirred at 0 - 5 ºC for 5 h and then evaporated under vacuum to dryness. The residue was purified by column chromatography eluting with a mixture of dichloromethane and hexane (1:1).

The diazonium salt solution previously prepared (0.86 mmol) was added drop wise to the solution of pyrrole **8** (1 mmol) and pyridine (1mL, 1.25 mmol) in methanol (20 mL). The combined solution was maintained at 0 - 5 ºC for 5 h while stirred. After this time the resulting mixture was evaporated under vacuum to dryness. The residue was purified by column chromatography eluting with a mixture of dichloromethane and hexane (1:1).

1-(1-(4-Methoxyphenyl)-1*H*-pyrrol-2-yl)-2-(thiazol-2-yl)diazene (**9b).** Orange oil (73 mg, 30%). ^{1}H NMR ($CDCl_3$) δ 3.89 (s, 3H, OCH_3), 6.55-6.57 (m, 1H, 4'-H), 7.02 (d, 2H, *J*=9.3 Hz, 3''-H and 5''-H), 7.18-7.20 (m, 2H, 3'-H and 5'-H), 7.35-7.41 (m, 3H, 4-H, 2''-H and 6''-H), 7.87 (d, 1H, *J*=3.6 Hz, 3-H). λ_{max}(Dioxane)/nm 419 (ε/dm^3 mol^{-1} cm^{-1} 17,600). IR (Liquid film) ν/ cm^{-1} 2965, 1731, 1407, 1339, 1304, 1243, 1216, 1170, 1141, 996, 898, 828, 743, 728. MS (EI$^+$): *m/z* (%) = 285 ([M+1]$^+$, 93), 264 (10). HMRS: *m/z* (EI$^+$): for $C_{14}H_{12}N_4OS$, calcd. 285.0800, found 285.0805.

1-(1-(4-Methoxyphenyl)-1*H*-pyrrol-2-yl)-2-phenyl)diazene (**10a).** Orange oil (205 mg, 85%). ^{1}H NMR ($CDCl_3$) δ 3.90 (s, 3H, OCH_3), 6.45-6.48 (m, 1H, 4'-H) 6.95-6.96 (m, 1H, 5'-H), 7.00 (d, 2H, *J*=9.0 Hz, 3''-H and 4''-H), 7.19-7.21 (m, 1H, 3'-H), 7.27-7.43 (m, 5H, 3-H, 4-H, 5-H, 2''-H, and 5''-H), 7.70-7.73 (m, 2H, 2-H and 6-H). ^{13}C NMR ($CDCl_3$) δ 55.5, 99.9, 111.1, 113.9, 122.2, 127.0, 127.3, 128.9, 129.5, 131.8, 146.6, 153.0, 158.7. λ_{max}(Dioxane)/nm 386 (ε/dm^3 mol^{-1} cm^{-1} 15,700). IR (Liquid film) ν/ cm^{-1} 2957, 2934, 2908, 2836, 2053, 1879, 1632, 1612, 1589, 1515, 1480, 1463, 1454, 1442,1301, 1250, 1202, 1109, 1093, 1071, 1035, 996, 913, 872, 832, 801. MS (EI): *m/z* (%) = 277 (M$^+$, 100), 276 (65), 172 (51), 157 (17). HMRS: *m/z* (EI) for $C_{17}H_{15}N_3O$, calcd. 277.1215, found 277.1210.

Azo pyrroles **10b-c** were synthesized through azo coupling of pyrrole **8** with aryl-diazonium salts **4b-c** using the same experimental procedure described above in sub-section 1.1 and 1.2.

1-(1-(4-Methoxyphenyl)-1*H*-pyrrol-2-yl)-2-(4-cyanophenyl)diazene (**10b).** Dark green solid (283 mg, 94%). Mp 126-128 ºC. ^{1}H NMR ($CDCl_3$) δ 3.89 (s, 3H, OCH_3), 6.48-6.50 (m, 1H, 4'-H), 6.93 (dd, 1H, *J*=5.6 and 2Hz, 5'-H), 7.00 (d, 2H, *J*=9.0 Hz, 3''-H and 5''-H), 7.26-7.27 (m, 1H, 3'-H), 7.39 (d, 2H, *J*=9.0 Hz, 2''-H and 6''-H), 7.65-7.73 (m, 4H, 2, 3, 5 and 6-H). ^{13}C NMR ($CDCl_3$) δ 55.5, 101.0, 111.7, 114.0, 118.9, 122.6, 127.3, 128.6, 131.3, 133.0, 147.0, 155.7, 158.9. λ_{max}(Dioxane)/nm 404 (ε/dm^3 mol^{-1} cm^{-1} 19,880). IR (Liquid film) ν/ cm^{-1}IR (Nujol) ν 2955, 2225, 1605, 1515, 1345, 1248, 1201, 1174, 1033, 833, 728 cm^{-1}. MS (EI$^+$) *m/z* (%): 302 (M$^+$, 100), 301 (60), 172 (68), 118 (38). HMRS: *m/z* (EI$^+$) for $C_{18}H_{14}N_4O$; calcd: 302.1168; found: 302.1169.

1-(1-(4-Methoxyphenyl)-1*H*-pyrrol-2-yl)-2-(4-nitrophenyl)diazene (**10c).** Brown solid (306 mg, 95%). Mp 173-174 ºC. ^{1}H NMR ($CDCl_3$) δ 3.83 (s, 3H, OCH_3), 6.57-6.59 (m, 1H, 4'-H), 6.94 (dd, 1H, *J*=4.4 and 1.5 Hz, 5'-H), 7.09 (d, 2H, *J*=9.0 Hz, 3''-H and 5''-H), 7.50

(d, 2H, *J*=9.0 Hz, 2''-H and 6''-H), 7.69-7.70 (1H, m, 3'-H), 7.74 (d, 2H, *J*=9.0 Hz, 2-H and 6-H), 8.30 (d, 2H, *J*=9.0 Hz, 3-H and 5-H). ^{13}C NMR (DMSO -d_6) δ 55.5, 101.6, 112.3, 114.2, 122.4, 125.1, 127.4, 130.7, 146.8, 147.0, 147.1, 156.7, 158.6. λ_{max}(Dioxane)/nm 417 (ε/dm^3 mol^{-1} cm^{-1} 17,600). IR (liquid film) ν/ cm^{-1} 2955, 1197, 1168, 1033, 892, 834, 771, 722. MS (EI) *m/z* (%): 322 (M$^+$, 30), 292 (100), 172 (34). HMRS: *m/z* (EI) for $C_{17}H_{14}N_4O_3$; calcd: 322.1066; found: 322.1070.

4.5. Instruments

NMR spectra were obtained on a Varian Unity Plus Spectrometer at an operating frequency of 300 MHz for ^{1}H NMR and 75.4 MHz for ^{13}C NMR or a Bruker Avance III 400 at an operating frequency of 400 MHz for ^{1}H NMR and 100.6 MHz for ^{13}C NMR using the solvent peak as internal reference at 25 ºC. All chemical shifts are given in ppm using δ_H Me_4Si = 0 ppm as reference and *J* values are given in Hz. Assignments were made by comparison of chemical shifts, peak multiplicities and *J* values and were supported by spin decoupling-double resonance and bidimensional heteronuclear HMBC and HMQC correlation techniques. IR spectra were determined on a BOMEM MB 104 spectrophotometer using KBr discs. UV-visible absorption spectra (200 – 800 nm) were obtained using a Shimadzu UV/2501PC spectrophotometer. Mass spectrometry analyses were performed at the "C.A.C.T.I. -Unidad de Espectrometria de Masas" at the University of Vigo, Spain. Thermogravimetric analysis of samples was carried out using a TGA instrument model Q500 from TA Instruments, under high purity nitrogen supplied at a constant 50 mL min^{-1} flow rate. All samples were subjected to a 20 ºC min^{-1} heating rate and were characterized between 25 and 500 ºC. All melting points were measured on a Gallenkamp melting point apparatus and are uncorrected. Cyclic voltammetry (CV) was performed using a potentiostat/galvanostat (AUTOLAB /PSTAT 12) with the low current module ECD from ECO-CHEMIE and the data analysis processed by the General Purpose Electrochemical System software package also from ECO-CHEMIE. Three electrode-two compartment cells equipped with vitreous carbon-disc working electrodes, a platinum-wire secondary electrode and a silver-wire pseudo-reference electrode were employed for cyclic voltammetric measurements. The concentration of the compounds were 1 mmol dm^{-3} and 0.1 mol dm^{-3} [NBu_4][BF_4] was used as the supporting electrolyte in dry *N*,*N*-dimethylformamide solvent. The cyclic voltammetry was conducted usually at 0.1 Vs^{-1}, or at different scan rates (0.02-0.50 Vs^{-1}), for investigation of scan rate influence. The potential is measured with respect to ferrocinium/ferrocene as an internal standard.

4.6. Solvatochromic study

The solvatochromic study was performed using 10^{-4} M solutions of dyes **5-7** and **9-10** in several solvents at room temperature.

4.7. Photochromic measurements

For measurements of λ_{max}, A_{eq} and k_{Δ} under continuous visible irradiation, 2.0×10^{-5} M acetone solutions were used. Irradiation experiments were made using a CARY 50 Varian spectrophotometer coupled to a 150W ozone free xenon lamp (6255 Oriel Instruments). The light from the UV–vis lamp was filtered using a water filter (61945 Oriel Instruments) and a long-pass filter (Schott GG 420) at 20 ºC and carried to the spectrophotometer holder, perpendicular to the monitoring beam using a fibre-optic system (77654 Oriel Instruments). A thermostated (20 ºC) 10 mm quartz cell containing the sample solution (3.5 mL) and equipped with magnetic stirring was used. Three spectrokinetic parameters, normally quoted when describing the properties of photochromic compounds, were evaluated: maximum wavelength of absorption (λ_{max}), thermal colouration rates (k_{Δ}) and maximum absorbance attained at λ_{max} (A_{max}). The colouration kinetics was then studied in the dark. The thermal coloration curves were analysed evaluating the fitting of the experimental data to the mono-exponential equation:

$$A(t) = A_1 e^{-kt} + A_0$$

where $A(t)$ is the absorbance at λ_{max} at any instant t, A_1 a proportional factor, k the thermal colouration rate and A_0 the absorbance in the dark when time approaches infinity. The model was found to accurately fit our data when the quadratic residual errors were 10^{-6} or less.

Nonlinear optical measurements using the hyper-Rayleigh scattering (HRS) method[27]

Hyper-Rayleigh scattering (HRS) was used to measure the first hyperpolarizability β of response of the molecules studied. The experimental set-up for hyper-Rayleigh measurements is similar to the one presented by Clays et al. [27] The incident laser beam came from a Q-switched Nd:YAG laser operating at a 10 Hz repetition rate with approximately 10 mJ of

energy per pulse and a pulse duration (FWHM) close to 12 ns at the fundamental wavelength of 1064 nm. The incident power could be varied using a combination of a half wave-plate and Glan polarizer. The incident beam was weakly focused (beam diameter ~0.5 mm) into the solution contained in a 5 cm long cuvette. The hyper- Rayleigh signal was collimated using a high numerical aperture lens passed through an interference filter centred at the second harmonic wavelength (532 nm) before being detected by a photomultiplier (Hamamatsu model H9305-04). The current pulse from the photomultiplier was integrated using a Stanford Research Systems gated box-car integrator (model SR250) with a 25 ns gate centred on the temporal position of the incident laser pulse. The hyper-Rayleigh signal was normalized at each pulse using the second harmonic signal from a 1 mm quartz plate to compensate for fluctuations in the temporal profile of the laser pulses due to longitudinal mode beating. Dioxane was used as a solvent, and the β values were calibrated using a reference solution of *p*-nitroaniline (*p*NA) [28] also dissolved in dioxane at a concentration of 1 x 10^{-2} mol dm^{-3} (external reference method). The hyperpolarizability of *p*NA dissolved in dioxane is known from EFISH measurements carried out at the same fundamental wavelength. The concentrations of the solutions under study were chosen so that the corresponding hyper-Rayleigh signals fell well within the dynamic range of both the photomultiplier and the box-car integrator. All solutions were filtered (0.2 μm porosity) to avoid spurious signals from suspended impurities. The small hyper Rayleigh signal that arises from dioxane was taken into account according to the expression

$$I_{2\omega} = G\left(N_{solvent}\left\langle\beta^2_{solvent}\right\rangle + N_{solute}\left\langle\beta^2_{solute}\right\rangle\right)I^2_{\omega}$$

where the factor G is an instrumental factor that takes into account the detection efficiency (including geometrical factors and linear absorption or scattering of the second harmonic light on its way to the detector) and local field corrections.

We took particular care to avoid reporting artificially high hyperpolarizibilities due to a possible contamination of the hyper Rayleigh signal by molecular fluorescence near 532 nm. Measurements were carried out using two different interference filters with different transmission pass bands centred near the second harmonic at 532 nm. The transmission band of the narrower filter (CVI model F1.5-532-4) was 1.66 nm (full width at half maximum) with a transmission of 47.6% at the second harmonic, while the corresponding values for the wider filter (CVI model F03-532-4) were 3.31 nm, with a transmission of 63.5% at the second

harmonic. The transmission of each filter at the second harmonic wavelength was carefully determined using a crystalline quartz sample. We assume that any possible fluorescence emitted from the solutions is essentially constant over the transmission of both interference filters. Then by comparing the signals obtained with the two different filters we can determine the relative contributions of the hyper-Rayleigh and possible fluorescence signals. The relevant equations are:

$$S_{NB}^{2\omega} = \left(\frac{S_{NB}A_{WB} - S_{WB}A_{NB}}{T_{NB}A_{WB} - T_{WB}A_{NB}} \right) T_{NB}$$

$$S_{NB}^{F} = \left(\frac{S_{LB}T_{NB} - S_{NB}T_{LB}}{T_{NB}A_{WB} - T_{WB}A_{NB}} \right) A_{NB}$$

Here $S_{NB}^{2\omega}$ is the hyper Rayleigh scattering contribution to the signal, i.e. the signal that would have been measured using the "narrow" band filter if there were no fluorescence present. The fluorescence contribution to the signal measured using the narrow band interference filter is S_{NB}^{F}. The signals S_{NB} and S_{WB} are the actual signals measured (after correction for the solvent contribution) using the "narrow" (CVI model F1.5-532-4) and "wide" (CVI model F03-532-4) band interference filters. The transmissions T_{NB} and T_{WB} are respectively the transmission of the "narrow" and "wide" band interference filters at the second harmonic wavelength (47.6% and 63.5%), A_{NB} and A_{WB} represent the area under the respective filter's transmission curve. The respective transmission curves were obtained using a dual-beam spectrophotometer with slits adjusted to give 0.1 nm resolution. We obtained values of 1.29 nm and 2.18 nm for A_{NB} and A_{WB} respectively.

Acknowledgements

Thanks are due to the *Fundação para a Ciência e Tecnologia* (Portugal) and FEDER for financial support through the Centro de Química and Centro de Física- Universidade do Minho, Project PTDC/QUI/66251/2006 (FCOMP-01-0124-FEDER-007429), Project PTDC/CTM/105597/2008 with funding from COMPETE/FEDER and research grants to M. C. R. Castro (UMINHO/BI/142/2009) and M. F. S. Cardoso (UMINHO/BII/249/2009). The NMR spectrometer Bruker Avance III 400 is part of the National NMR Network and was purchased within the framework of the National Program for Scientific Re-equipment, contract REDE/1517/RMN/2005 with funds from POCI 2010 (FEDER) and FCT.

References and notes

[1] (a) Zyss DS. In: Non linear optical properties of organic molecules and crystals, vol. 1 and vol. 2. Orlando: Academic Press; 1987;

(b) Prasad PN, Williams DJ. In: Introduction to Nonlinear Optical Effects in Molecules and Polymers. New York: Wiley-VCH; 1991, p. 132-174;

(c) Kanis DR, Ratner MA, Marks TJ. Chem Rev 1994;94:195;

(d) Marder SR, Kippelen B, Jen AKY, Peyghambarian N. Nature 1997;388:845;

(e) Shi Y, Zhang YQC, Zhang H, Bechtel JH, Dalton LR, Robinson BH, Steier WH. Science 2000;288:119.

[2] For some examples see: (a) Cheng LT, Tam W, Marder SR, Steigman AE, Rikken G, Spangler CW. J Phys Chem 1991;95:10643;

(b) Dalton LR, Harper AW, Ghosn R, Steier WH, Ziari M, Fetterman H, Shi Y, Mustacich RV, Jenand AK-Y, Shea KJ. Chem Mater 1995;7:1060;

(c) Wong MS, Bosshard C, Pan F, Günter P. Adv Mater 1996;8:677;

(d) Blanchard-Desce M, Alain V, Bedworth PV, Marder SR, Fort A, Runser C, Barzoukas M, Lebus S, Wortmann R. Chem Eur J 1997;3:1091;

(e) Verbiest T, Houbrechts S, Kauranen M, Clays K, Persoons A. J Mater Chem 1997;7:2175.

[3] (a) Dirk CW, Katz HE, Schilling ML, King LA. Chem Mat 1990;2:700;

(b) Rao VP, Jen AK-Y, Wong KY, Drost KJ. Tetrahedron Lett 1993;34:1747;

(c) Jen AK-Y, Rao VP, Wong KY, Drost KJ. J Chem Soc Chem Commun 1993;90;

(d) Rao VP, Jen AK-Y, Wong KY, Drost KJ. J Chem Soc Chem Commun 1993;1118;

(e) Miller RD, Lee VY, Moylan CR. Chem Mat 1994;6:1023;

(f) Abbotto A, Bradamante S, Pagani GA. J Org Chem 1996;61:1761;

(g) Chou S-SP, Sun D-J, Lin H-C, Yang P-K. Tetrahedron Lett 1996;37:7279;

(h) Shu C-F, Tsai W-J, Chen J-Y, Jen AK-Y, Zhang Y, Chen T-A. J Chem Soc Chem Commun 1996;2279;

(i) Shu C-F, Wang Y-K. J Mater Chem 1998;8:833;

(j) Wang Y-K, Shu C-F, Breitung EM, McMahon RJ. J Mater Chem 1999;9:1449;

(k) Facchetti A, Abbotto A, Beverina L, van der Boom ME, Dutta P, Evmenenko G, Marks TJ, G. Pagani A. Chem Mat 2002;14:4996;

(l) Facchetti A, Abbotto A, Beverina L, M. E. van der Boom, Dutta P, Evmenenko G, Pagani GA, Marks TJ. Chem Mater 2003;15:1064;

(m) Audebert P, Kamada K, Matsunaga K, Ohta K. Chem Phys Lett 2003;367:62;

(n) Facchetti A, Beverina L, van der Boom ME, Dutta P, Evmenenko G, Pagani GA, Marks TJ. J Am Chem Soc 2006;128:2142 and references cited therein;

(o) Davies JA, Elangovan A, Sullivan PA, Olbricht BC, Bale DH, Ewy TR, Isborn CM, Eichinger BE, Robinson BH, Reid PJ, Li X, Dalton LR. J Am Chem Soc 2008;130:10565;

(p) Abbotto A, Beverina L, Manfredi N, Pagani GA, Archetti G, Kuball H-G, Wittenburg C, Heck J, Holtmann J. Chem Eur J 2009;15:6175.

[4] (a) Varanasi PR, Jen AK-Y, Chandrasekhar J, Namboothiri INN, Rathna A. J Am Chem Soc 1996;118:12443;

(b) Albert IDL, Marks TJ, Ratner MA. J Am Chem Soc 1997;119:6575;

(c) Breitung EM, Shu C-F, McMahon RJ. J Am Chem Soc 2000;122:1154.

[5] (a) Raposo MMM, Sousa AMRC, Kirsch G, Ferreira F, Belsley M, Matos Gomes E, Fonseca AMC. Org Lett 2006;8:3681;

(b) Batista RMF, Costa SPG, Malheiro EL, Belsley M, Raposo MMM. Tetrahedron 2007;63:4258;

(c) Batista RMF, Costa SPG, Belsley M, Raposo MMM. Tetrahedron 2007;63:9842;

(d) Pina J, Seixas de Melo S, Batista RMF, Costa SPG, Raposo MMM. Phys Chem Chem Phys 2010;12:9719.

[6] Yager KG, Barrett CJJ. Photochem Photobiol A Chem 2006;182:250.

[7] (a) Towns AD, Dyes Pigm 1999;42:3 and references cited therein;

(b) Yesodha SK, Pillai CKS, Tsutsumi N. Prog Polym Sci 2004;29:45 and references cited therein.

[8] (a) Åstrand P-O, Sommer-Larsen P, Hvilsted S, Ramanujam PS, Bak KL, Sauer SPA. Chem Phys Lett 2000;325:115;

(b) Wang Y, Ma J, Jiang Y. J Phys Chem A 2005;109:7197;

[9] Nabeshima Y, Shishido A, Kanazawa A, Shiono T, Ikeda T, Hiyama T. Chem Mater 1997;9:1480;

[10] Zhu Z, Wang Y, Lu Y. Macromolecules 2003;36:9585.

[11] (a) Zollinger H. In: Color Chemistry, ch. 7. New York: VCH Publishers, Inc; 1991;

(b) Rau H. In: Dürr H, Bouas-Laurent H, editors. Photochromism: Molecules and Systems, ch. 4. Amsterdam: Elsevier; 1990;

(c) Bouas-Laurent H, Dürr H. Pure Appl Chem 2001;73:639;

(d) Blinov LM, Kozlovsky MV, Ozaki M, Yoshino K. Mol Cryst Liq Cryst Sci Technol Sect C 1996;6:235.

[12] Trofimov BA, Schmidt EY, Mikhaleva AI, Vasiltsov AM, Zaitsev AB, Smolyanina NS, Senotrusova EY, Afonin AV, Ushakov IA, Petrushenko KB, Kazheva ON, Dyachenko OA, Smirnov VV, Schmidt AF, Markova MV, Morozova L. Eur J Org Chem 2006;4021.

[13] (a) Raposo MMM, Sousa AMRC, Fonseca AMC, Kirsch G. Tetrahedron 2005;61:8249;
(b) Raposo MMM, Sousa AMRC, Fonseca AMC, Kirsch G. Mater Sci Forum 2006;514-516:103;
(c) Coelho PJ, Carvalho LM, Fonseca AMC, Raposo MMM. Tetrahedron Lett 2006;47:3711.

[14] (a) Raposo MMM, Ferreira AMFP, Belsley M, Moura JCVP. Tetrahedron 2008;64:5878;
(b) Raposo MMM, Ferreira AMFP, Belsley M, Matos Gomes E, Moura JCVP. Mater Sci Forum 2008;587-588:268.

[15] (a) Raposo MMM, Ferreira AMFP, Amaro M, Belsley M, Moura JCVP. Dyes Pigments 2009;83:59;
(b) Coelho PJ, Carvalho LM, Moura JCVP, Raposo MMM. Dyes Pigments 2009;82:130;
(c) Otsuki J, Suwa K, Narutaki K, Sinha C, Yoshikawa I, Araki K. J Phys Chem A 2005;109:8064;
(d) Brown E, Granneman G. J Am Chem Soc 1975;97:621;
(e) Barachevsky VA, Oliveira-Campos AMF, Stebunova LV, Chudinova LV, Avakyan VG, Maslyanitsyn IA, Shigorin VD. Zhurnal Nauchii Prikladnoi Fotografii 2002;47:4.

[16] (a) Raposo MMM, Sampaio AMBA, Kirsch G. Synthesis 2005;2:199;
(b) Raposo MMM, Sampaio AMBA, Kirsch G. Tetrahedron 2006;62:3493.

[17] Jackson AH. In: Jones RA, editor. The Chemistry of Heterocyclic Compounds, vol. 48, part 1. New York: Wiley; 1990. p. 295.

[18] (a) Butler AR, Pogorzelec P, Shepherd PT. J Chem Soc Perkin Trans II 1977;1452;
(b) Boukou-Poba J-P, Farnier M, Guilard R. Tetrahedron Lett 1979;20:1717;
(c) Trofimov BA, Sobenina LN, Demenev AP, Mikhaleva AI, Ushakov IA, Tarasova OA, Smirnov VI, Petrushenko KB, Vokin AI, Murzina NM, Myachina GF. Arkivok 2001;ix:37;
(d) Raposo MMM, Sousa AMRC, Kirsch G, Ferreira F, Belsley M, Matos Gomes E, Fonseca AMC. Tetrahedron 2005;61:11991.

[19] (a) Hallas G, Towns AD. Dyes Pigments 1997;33:205;
(b) Hallas G, Towns AD. Dyes Pigments 1997;34:133.

[20] See for example: (a) Effenberger F, Würthner F, Steybe F. J Org Chem 1995;60:2082;
(b) Raposo MMM, Fonseca AMC, Kirsch G. Tetrahedron 2004;60:4071;

(c) Oliva MM, Casado J, Raposo MMM, Fonseca AMC, Hartmann H, Hernandez V, Navarrete JTP. J Org Chem 2006;71:7509;

(d) Herbivo C, Comel A, Fonseca AMC, Kirsch G, Belsley M, Raposo MMM. Dyes Pigments 2010;82:217.

[21] a) Kamlet MJ, Abboud J-LM, Abraham MH, Taft RW. J Org Chem 1983;48:2877;

(b) Kamlet MJ, Abboud J-LM, Abraham MH, Taft RW. J Am Chem Soc 1977;99:6027.

[22] See for example. (a) Bossard G, Knöpfle P, Prêtre P, Günter P. J Appl Phys 1992;71:1594;

(b) Kim O-K, Fort A, Barzoukas M, Blanchard-Desce M, Lehn J-M. J Mater Chem 1999;9:2227 and references cited.

[23] McCormac T, Farrell D. Electrochim Acta 2001;46:3287.

[24] Dufresne S, Bourgeaux M, Skene W,G. J Mater Chem 2007;17:1166.

[25] (a) Cihaner A, Algi F. Electrochim Acta 2009;54:1702;

(b) Audebert P, Sadki S, Miomandre F, Hapiot P, Ching KC. New J Chem 2003;27:798.

[26] O'Connor MJ, Yelle RB, Linz TM, Haley MM. C R Chim 2009;12:385.

[27] (a) Clays K, Persoons A. Rev Sci Instrum 1992;63:3285;

(b) Clays K, Persoons A. Phys Rev Lett 1991;66:2980.

[28] (a) Teng CC, Garito AF. Phys Rev B 1983;28:6766;

(b) Stahelin M, Burland DM, Rice JE. Chem Phys Lett 1992;191:245.

[29] (a) Oudar JL J. Chem Phys 1977;67:446;

(b) Oudar JL, Chemla DS. J Chem Phys 1977;66:2664;

(c) Zyss J, Oudar JL. Phys Rev A 1982;26:2016.

[30] Li Y, Patrick BO, Dolphin D. J Org Chem 2009;74:5237.

Captions

Scheme 1. Photochemical $E \rightarrow Z$ isomerization of aromatic azo dyes.

Scheme 2. Synthesis of thienylpyrrole azo dyes **5**-**7** through azo coupling reaction of thienylpyrroles **1** with thiazolyldiazonium salts **2** and **3** and aryldiazonium salt **4a**.

Scheme 3. Synthesis of pyrrole azo dyes **9b** and **10a**-**c** through azo coupling reaction of pyrrole **8** with thiazolyldiazonium salt **2** and aryldiazonium salts **4a**-**c**.

Table 1. Solvatochromic data [λ_{max} (nm) and υ_{max} (cm^{-1}) of the charge-transfer band] for thienylpyrrole **5-7** and pyrrole azo dyes **9-10** in 4 solvents with π^* values by Kamlet and Taft [21].

Table 2. Electrochemical data for compounds **5-10**

[a] Measurements made in dry DMF containing 1.0 mM in each compounds and 0.10 M $[NBu_4][BF_4]$ as base electrolyte at a carbon working electrode with a scan rate of 0.1 V s^{-1}. All E values are quoted in volts *versus* the ferrocinium/ferrocene-couple. $E_{1/2}$ corresponds to the reversible process. E_{pc} and E_{pa} correspond to the cathodic and anodic peak potentials, respectively.

[b] E_{HOMO} = 4.39 + E_{ox} (eV) and E_{LUMO} = E_{red} + 4.39 (eV).

Table 3. UV-vis absorptions, β and β_0 values and T_d data for thienylpyrrole **5-7** and pyrrole azo dyes **9b** and **10a-c**[a].

[a] Experimental hyperpolarizabilities and spectroscopic data measured in dioxane solutions.

[b] All the compounds are transparent at the 1064 nm fundamental wavelength.

[c] Data corrected for resonance enhancement at 532 nm using the two-level model with $\beta_0 = \beta [1-(\lambda_{max}/1064)^2][1-(\lambda_{max}/532)^2]$; damping factors not included 1064 nm [29].

[d] Decomposition temperature (T_d) measured at a heating rate of 20 ºC min^{-1} under a nitrogen atmosphere, obtained by TGA.

[e] It was not possible to measure the β due to the high amount of fluorescence.

[f] Compounds **7a**, **9b** and **10a** were obtained as oils.

Table 4 Spectrokinetic properties under continuous visible irradiation: maximum wavelength of absorption (λ_{max}), maximum absorbance (A_{max}), absorbance variation (ΔAbs), thermal colouration rates (k_Δ) and half-time life ($t_{1/2}$) of azo dyes **5a**–**f**, **6b**, **7a**, **10a-c**, and **11c** in acetone.

Figure 1. Structure of diazene thienylpyrroles **11b-c [**13a-b].

Figure 2. Cyclic voltammogram of compound **5d** ($1.0x10^{-3}$ mol dm^{-3}) in DMF, 0.1 mol dm^{-3} $[NBu_4][BF]_4$ at a vitreous carbon electrode. **a** - between -0.50 V and -2.30 V *vs.* fc^+/fc, scan rate 0.1 Vs^{-1}; **b** - between - 0.50 V and -1.70 V, scans rate 0.02, 0.05, 0.20 and 0.30 Vs^{-1}; **c** - between -0.50 V and 0.80 V *vs.* fc^+/fc, scan rate 0.1 Vs^{-1}.

Figure 3. Thermal analysis data for azo dye **5a** through TGA recorded under a nitrogen atmosphere, measured at a heating rate of 20 ºC min^{-1}.

Figure 4. Absorption spectra of dye **5a** under visible irradiation (-----) and in the dark (——) in acetone.

Figure 5. Visible irradiation/dark cycles for azo dyes **5a** and **7a.**

Figures

Figure 1

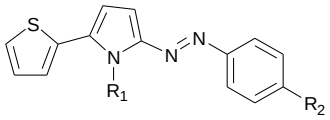

11b R_1 = 4-$MeOC_6H_4$, R_2 = CN
11c R_1 = 4-$MeOC_6H_4$, R_2 = NO_2

<Figure 2>

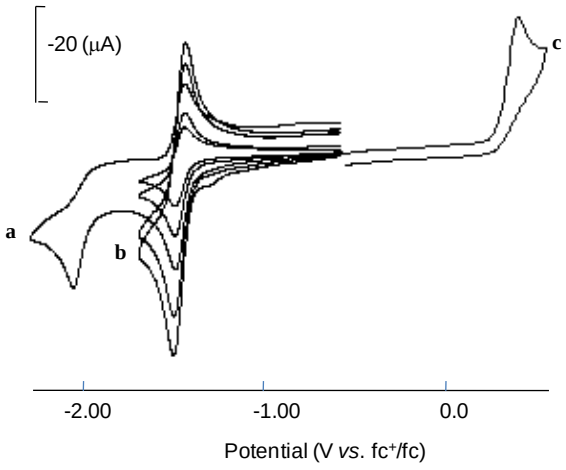

<Figure 3>

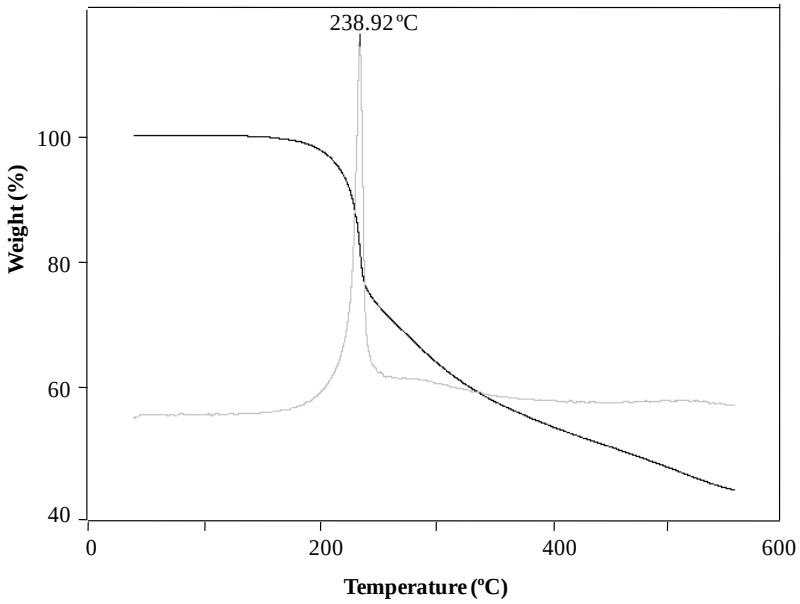

<Figure 4>

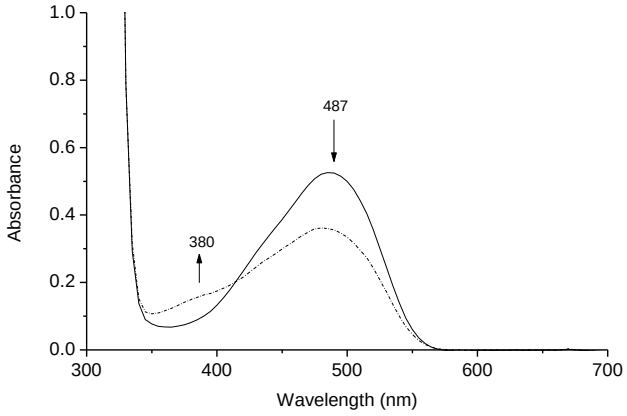

<Figure 5>

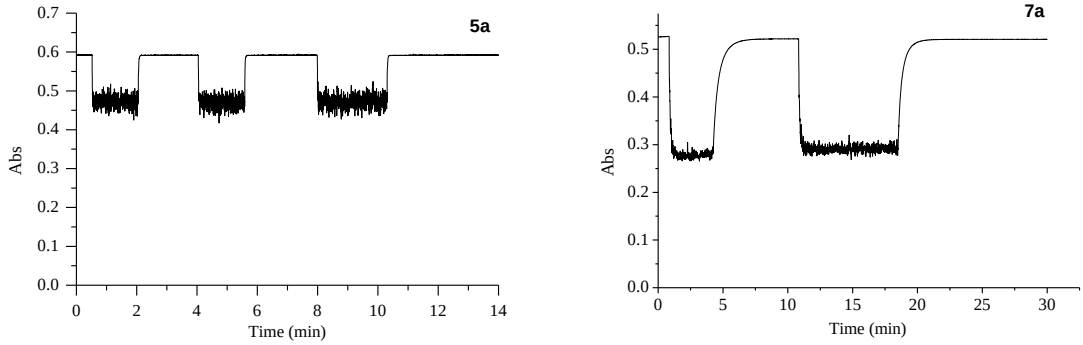
5a
Abs
Time (min)
0.0
0.1
0.2
0.3
0.4
0.5
0.6
0.7
0
2
4
6
8
10
12
14
7a
Abs
Time (min)
0.0
0.1
0.2
0.3
0.4
0.5
0
5
10
15
20
25
30

Tables

<Table 1>

Compound	Solvent (π*)							
	Diethyl ether (0.54)		Ethanol (0.54)		1,4-Dioxane (0.55)		DMSO (1.00)	
	λ_{max}(nm)	ν_{max}(cm^{-1})	λ_{max}(nm)	ν_{max}($cm^{-1)}$	λ_{max}(nm)	ν_{max}(cm^{-1})	λ_{max}(nm)	ν_{max}(cm^{-1})
5a	477	20,964	491	20,367	486	20,576	498	20,080
5b	487	20,533	504	19,841	493	20,284	511	19,570
5c	488	20,491	506	19,763	497	20,121	514	19,455
5d	487	20,533	500	20,000	494	20,243	512	19,531
5e	483	20,704	499	20,040	491	20,367	509	19,646
5f	482	20,747	498	20,080	489	20,450	504	19,841
6b	488	20,491	505	19,801	498	20,080	513	19,493
7a	413	24,213	416	24,038	419	23,866	426	23,474
9b	414	24,154	417	23,980	419	23,866	427	23,419
10a	384	26,041	386	25,906	386	25,906	390	25,641
10b	402	24,875	406	24,630	404	24,752	411	24,330
10c	413	24,213	417	23,980	417	23,980	429	23,331

<Table 2>

Compound	Reduction [a]		Oxidation [a]	Band gap(eV) [b]
	$-{}^{1}E_{1/2}$(V)	$-{}^{2}E_{pc}$(V)	E_{pa}(V)	
5a	1.51	2.25	0.59	2.10
5b	1.50	2.16	0.57	2.07
5c	1.48	2.11	0.58	2.06
5d	1.53	2.27	0.60	2.13
5e	1.46	2.14	0.62	2.08
5f	1.46	2.10	0.62	2.08
6b	1.55	2.25	0.53	2.08
7a	1.95	__	0.56	2.51
8	__	__	0.86	__
9b	1.53	__	0.69	2.22
10a	1.90	__	0.76	2.66
10b	1.59	__	0.79	2.38
10c	1.30	1.93	0.81	2.11
11b [13a]	1.74	__	0.59	2.33
11c [13a]	1.35	1.83	0.62	1.97

<Table 3>

Entry	Azo dye	λ_{max}(nm)	β^{b}(10^{-30}esu)	β_0^{c}(10^{-30}esu)	T_d^{d}(ºC)
1	**5a**	486	164	21±15	239
2	**5b**	493	156	16±6	259
3	**5c**	497	175	17±2	273
4	**5d**	494	129	14±2	220
5	**5e**	491	198	23±4	206
6	**5f**	489	190	23±4	206
	6b	498	274	27±5	227
7	**7a**	419	95	31±3	---[f]
8	**9b**	419	80	26±6	---[f]
9	**10a**	386	---[e]	---[e]	---[f]
10	**10b**	404	84	30±11	216
11	**10c**	417	128	42±4	227
12	**11b**	473	345	58±2	288
13	**11c**	497	415	41±2	286
6	*p*NA	352	16.9 [28]	8.5	---

Table 4>

Azo dye	λ_{max} (nm)	A_{max}	ΔAbs	$k_{\Delta}(s^{-1})$ (%)	$t_{1/2}$ (s)
5a	487	0.592	0.121 (20.4%)	1.4 (98)	0.5
				0.072 (2)	
5b	499	0.542	0.120 (22%)	0.62 (99)	1.1
				0.08 (1)	
5c	500	0.659	0.147 (20.5%)	1.3 (82)	0.65
				0.33 (18)	
5d	495	0.612	0.135 (22%)	1.1 (81)	0.75
				0.33 (19)	
5e	493	0.669	0.142 (21.2%)	0.97 (87)	0.82
				0.3 (13)	
5f	493	0.511	0.100 (19.6%)	0.63 (100)	1.1
6b	499	0.459	0.036 (7.8%)	1.25 (97)	0.83
				0.031 (3)	
7a	420	0.523	0.277 (53%)	0.069 (43)	20
				0.026 (57)	
9b	420	0.38	0.19 (50%)	0.0193 (100)	36
10a	388	0.53	0.29 (54%)	5.2×10^{-4} (100)	1330
10b	405	0.472	0.31 (66%)	0.0028 (100)	237
10c	420	0.38	0.21 (55%)	0.0095 (100)	70
11c [13a]	500	0.42	0.11 (26)	0.33	2.1

Schemes

Scheme 1

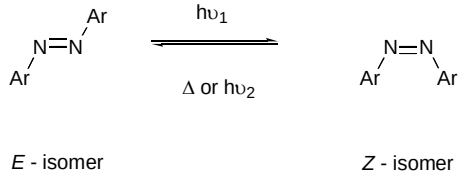

E - isomer

Z - isomer

<Scheme 2>

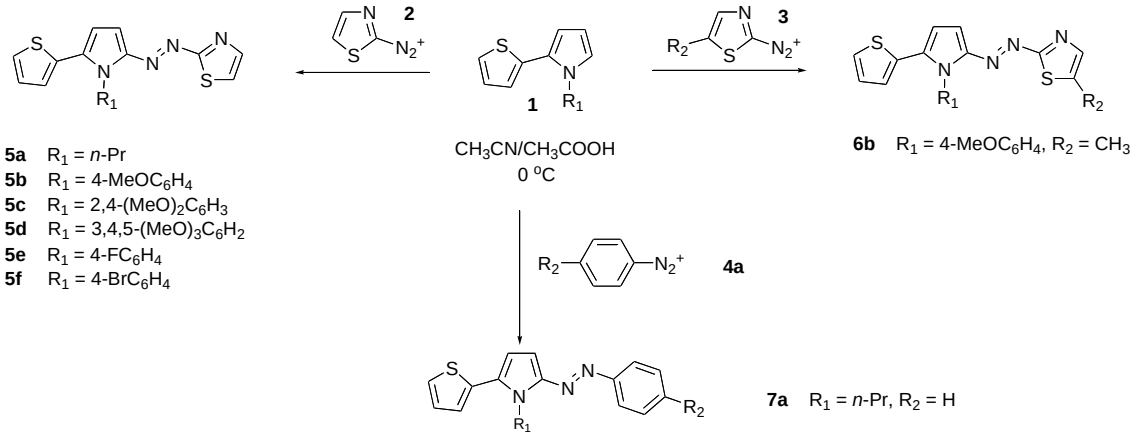

5a R_1 = *n*-Pr
5b R_1 = 4-$MeOC_6H_4$
5c R_1 = 2,4-$(MeO)_2C_6H_3$
5d R_1 = 3,4,5-$(MeO)_3C_6H_2$
5e R_1 = 4-FC_6H_4
5f R_1 = 4-BrC_6H_4

<Scheme 3>